Electromagnetic Diffraction by a Planar Array of Circular Disks*

W. H. EGGIMANN† AND R. E. COLLIN†, SENIOR MEMBER, IRE

Summary—The diffraction of a plane electromagnetic wave by a planar rectangular array of perfectly conducting circular disks is considered. The diffracted field is calculated from the induced electric and magnetic dipole moments and higher-order multipole moments. Static and dynamic interactions between the induced dipole moments are being considered, first by using a plane-wave approximation for the dipole fields (for cases where the separation of the disks is large compared with the wavelength) and then by calculating the actual fields at each disk. The formulas are applied to calculate the input susceptance of a disk-loaded rectangular waveguide. Satisfactory agreement with experimental results is obtained.

Introduction

IN A RECENT PAPER[1] the electromagnetic diffraction by a perfectly conducting circular disk was calculated. The induced surface current density was obtained as a power series in

(ka) $(k = 2\pi/\lambda$ = wave number, a = disk radius).

These results are now used to calculate the diffraction by a planar rectangular array of disks. Problems of this sort are important in the studies of artificial dielectrics where the molecular dipoles of real dielectrics are replaced by conductors distributed regularly or at random in a supporting medium. For many cases good approximate solutions have been found, usually for conductors with dimensions that are very small compared to the wavelength or for some very simple geometrical configurations. The case of an array of disks has been the object of early investigations. In a first approximation the disks are replaced by the induced electric and magnetic dipole moments which Bethe obtained during his studies of the diffraction by small holes.[2] Later the so-called static interaction, where phase differences between the oscillating dipole are neglected, was taken into account.

Here the formalism of the above-mentioned paper[1] is used to calculate the effect of higher order multipole moments and the dynamic interaction between the induced dipole moments of an array of circular disks, where it is recognized that the interaction fields are dipole fields. The mathematical development has to be rather sketchy. For more details the reader is referred to the original reports.[3,4]

It is desirable to relate the theoretical results to quantities which can be easily checked experimentally. As for any approximation, our results hold only for certain ranges of the parameters, in our case for small disks where $ka < 1$. Free space problems are usually not very amenable to experimental checks. It is therefore proposed to investigate a waveguide configuration which, by suitable arrangement, will turn out to be closely related to the free space problem.[5] This will be shown in the following section.

Shunt Susceptance of a Disk-Loaded Waveguide

Consider an arrangement of disks in a transverse plane of a rectangular waveguide as shown in Fig. 1. The disks are positioned such that their multiple images with respect to the guide walls form a planar regular rectangular array with spacings c and d. Similarly the TE_{10} mode corresponds to two symmetrical plane waves incident at angles $\theta_i = \pm\sin^{-1}\lambda/2g$ and polarized perpendicular to the plane of incidence as seen in Fig. 2. The reflected field at large distances is a TE_{10} mode only, traveling in the negative z direction, if the size of the guide can be chosen such that all other modes are cut off. That means that in the free space problem the disk array represents a perfect partially transparent reflector.

The reflected field can be calculated from the current distribution on the disks. The normalized fields for the TE_{10} mode are

$$\begin{aligned} \boldsymbol{e}_{10} &= -jkZ_0\left[\frac{2}{jghkZ_0\Gamma_{10}}\right]^{1/2}\cos(k_x x)\boldsymbol{a}_y \\ \boldsymbol{h}_{10} &= \Gamma_{10}\left[\frac{2}{jghkZ_0\Gamma_{10}}\right]^{1/2}\cos(k_x x)\boldsymbol{a}_x \\ \boldsymbol{h}_{z10} &= -k_x\left[\frac{2}{jghkZ_0\Gamma_{10}}\right]^{1/2}\sin(k_x x)\boldsymbol{a}_z \end{aligned} \tag{1}$$

* Received May 24, 1962. This work has been supported by the Electronics Research Directorate of the Air Force Cambridge Research Center, Bedford, Mass., under Contract No. AF 19(604)3887.

† Engineering Division, Case Institute of Technology, Cleveland, Ohio.

[1] W. H. Eggimann, "Higher order evaluation of electromagnetic diffraction by circular disks," IRE TRANS. ON MICROWAVE THEORY AND TECHNIQUES, vol. MTT-9, pp. 408–418; September, 1961.

[2] H. A. Bethe, "Theory of diffraction by small holes," *Phys. Rev.*, vol. 66, pp. 163–182; October, 1944.

[3] W. H. Eggimann, "Higher Order Evaluation of the Diffraction of Electromagnetic Fields by Circular Disks," Case Inst. of Tech., Cleveland, Ohio, Sci. Rept. No. 21, AF 19(604)3887; January, 1961.

[4] W. H. Eggimann, "Notes on Input Susceptance of a Disk Loaded Waveguide," Case Inst. of Tech., Cleveland, Ohio, Sci. Rept. No. 25, AF 19(604)3887; June, 1961.

[5] R. E. Collin, "A Note on Waveguide Image Techniques," Case Inst. of Tech., Cleveland, Ohio, Sci. Rept. No. 19, AF 19(604)3887; November, 1960.

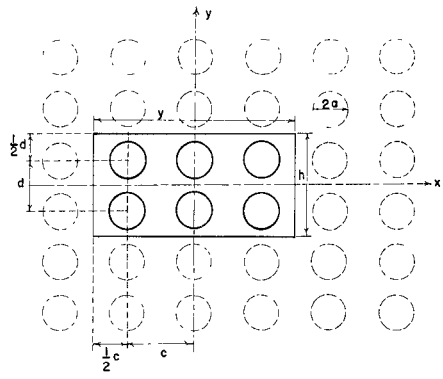

Fig. 1—Planar array of circular disks in a rectangular waveguide and their multiple images.

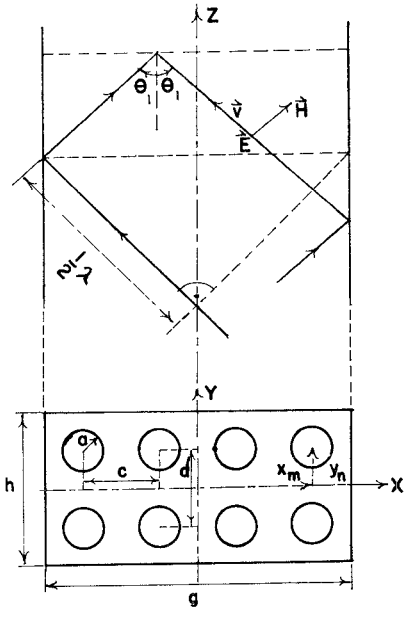

Fig. 2—Representation of the TE_{10} mode in a rectangular waveguide by two plane waves. The incident angle is given by $\theta_i = \sin^{-1} \lambda/2g$.

where

$$k_x = \frac{\pi}{g}, \qquad \Gamma_{10} = j\beta_{10} = (k_x^2 - k^2)^{1/2}.$$

We have further the orthogonality relation

$$\int_S \boldsymbol{e}_{10} \times \boldsymbol{h}_{z10} \cdot d\boldsymbol{S} = 1 \tag{2}$$

where the integration is over the cross section S of the waveguide.

The normalized transverse field moving in the negative z direction is

$$\begin{aligned} \boldsymbol{E}_{10}^- &= \boldsymbol{e}_{10} e^{\Gamma_{10} z} \\ \boldsymbol{H}_{10}^- &= -\boldsymbol{h}_{10} e^{\Gamma_{10} z} \end{aligned} \tag{3}$$

and in the positive z direction

$$\begin{aligned} \boldsymbol{E}_{10}^+ &= \boldsymbol{e}_{10} e^{-\Gamma_{10} z} \\ \boldsymbol{H}_{10}^+ &= \boldsymbol{h}_{10} e^{-\Gamma_{10} z}. \end{aligned} \tag{4}$$

The scattered dominant wave is

$$\begin{aligned} \boldsymbol{E}_{10}^s &= b_{10} \boldsymbol{E}_{10}^- \\ \boldsymbol{H}_{10}^s &= b_{10} \boldsymbol{H}_{10}^- \end{aligned} \tag{5}$$

where b_{10} is the scattering coefficient. b_{10} can be easily found by using the Lorentz reciprocity principle.[6]

$$b_{10} = -\frac{1}{2} \int_V \boldsymbol{E}_{10}^+ \cdot J dV. \tag{6}$$

The integral is taken over the volume V containing the induced current density.

A similar result holds for b_n of the nth scattered mode. Expansion of the mode $\boldsymbol{E}_n^+$ about the origin gives

$$\boldsymbol{E}_n^+(x, y) = \boldsymbol{E}_n^+(0) + x \frac{\partial \boldsymbol{E}_n^+}{\partial x} + y \frac{\partial \boldsymbol{E}_n^+}{\partial y} + \frac{1}{2}\left[x^2 \frac{\partial^2 \boldsymbol{E}_n^+}{\partial x^2} + 2xy \frac{\partial^2 \boldsymbol{E}_n^+}{\partial x \partial y} + y^2 \frac{\partial^2 \boldsymbol{E}_n^+}{\partial y^2}\right] + \cdots. \tag{7}$$

This leads to

$$\begin{aligned} -2b_n = \boldsymbol{E}_n^+ \cdot \int_V J dV &+ \left[\frac{\partial \boldsymbol{E}_n^+}{\partial x} \cdot \int_V x J dV + \frac{\partial \boldsymbol{E}_n^+}{\partial y} \cdot \int_V y J dV\right] \\ &+ \frac{1}{2}\left[\frac{\partial^2 \boldsymbol{E}_n^+}{\partial x^2} \cdot \int_V x^2 J dV + 2 \frac{\partial^2 \boldsymbol{E}_n^+}{\partial x \partial y} \cdot \int_V xy J dV \right. \\ &\left. + \frac{\partial^2 \boldsymbol{E}_n^+}{\partial y^2} \cdot \int_V y^2 J dV\right] + \cdots. \end{aligned} \tag{8}$$

In the following we consider the relation

$$\int_V V \cdot (\phi J) dV = \int_V (\phi V \cdot J + J \cdot V\phi) dV = \int_V \phi J \cdot d\boldsymbol{S} = 0 \tag{9}$$

which holds if the integration is taken over the total current distribution, because the component of J normal to the surface element $d\boldsymbol{S}$ must vanish. Hence

$$\int_V J \cdot V\phi dV = -\int_V \phi V \cdot J dV = j\omega \int_V \phi \rho_e dV \tag{10}$$

where ρ_e is the electric charge density.

First-Order Approximation

$$\begin{aligned} \int_V J dV &= \boldsymbol{a}_x \int_V Vx \cdot J dV + \boldsymbol{a}_y \int_V Vy \cdot J dV \\ &= \left[\boldsymbol{a}_x \int_V x \rho_e dV + \boldsymbol{a}_y \int_V y \rho_e dV\right] j\omega = j\omega \boldsymbol{P}^1 \end{aligned} \tag{11}$$

where $\boldsymbol{P}^1$ is by definition the electric dipole moment.

That gives

$$-2b_n^1 = \boldsymbol{E}_n^+ \cdot \int_V J dV = j\omega \boldsymbol{E}_n^+ \cdot \boldsymbol{P}^1. \tag{12}$$

[6] R. E. Collin, "Field Theory of Guided Waves," McGraw-Hill Book Co., Inc., New York, N. Y.; 1960.

where the superscript of the b_n^1 denotes the first-order approximation.

Second- and Third-Order Approximation

Using a similar procedure we find for the second- and third-order approximation

$$-2b_n^2 = j\omega(-\mu_0 \boldsymbol{H}_n^+ \cdot \boldsymbol{M} + \tfrac{1}{2}\nabla \boldsymbol{E}_n^+ : \overline{P}^2) \tag{13}$$

$$-2b_n^3 = j\omega(-\tfrac{1}{3}\mu_0 \nabla H_n^+ : \overline{Q} + \tfrac{1}{6}\nabla^2 \boldsymbol{E}_n^+ : \overline{P}^3) \tag{14}$$

where

$$\boldsymbol{M} = \frac{1}{2}\int r \times J dV = \text{magnetic dipole moment}$$

$$Q_{ij} = \int r_j (r \times J)_i dV = \int r_j (r_j J_k - r_k r_j) dV$$

$$P_{ij}^2 = \int r_i r_j \rho_e dV = \frac{1}{j\omega}\int (r_i J_j + r_j J_i) dV$$

electric quadrupole moment (15)

$$P_{ijk}^3 = \int r_i r_j r_k \rho_e dV = \frac{1}{j\omega}\int (r_i r_j J_k + r_j r_k J_i + r_k r_i J_j) dV$$

electric octupole moment.

The tensor products are defined as follows:

$$\nabla^n \boldsymbol{E}^+ : \overline{P}^n = \sum_{i,j,k\cdots=1}^{3} \frac{\partial^n E_i}{\partial r_j \partial r_k \cdots} P_{ijk\cdots}^n \tag{16}$$

and similarly for the magnetic moments. It has to be pointed out that $\overline{Q}$ is *not* the magnetic quadrupole moment. The total scattering coefficient is now

$$-b_n = \tfrac{1}{2}j\omega[\boldsymbol{E}_n^+ \cdot \boldsymbol{P}^1 - \mu_0 \boldsymbol{H}_n^+ \cdot \boldsymbol{M}^1 + \tfrac{1}{2}\nabla \boldsymbol{E}_n^+ : \overline{P}^2 - \tfrac{1}{3}\nabla H_n^+ : \overline{Q} + \tfrac{1}{6}\nabla^2 \boldsymbol{E}_n^+ : \overline{P}^3 \cdots]. \tag{17}$$

Using the theory of images we have an infinite array of disks and a plane wave incident at angles $\phi_i = 90°$ and $\theta_i = \sin^{-1}\lambda/2g$ (Fig. 2). The total scattered field is found by calculating and adding the contributions of the electric and magnetic dipole moments and multipole moments of all the disks.

The incident electric field has only a y component and is given by

$$E_{10y}^{\text{inc}} = E_0 \cos(k_x x) e^{-\Gamma_{10} z}. \tag{18}$$

From (5) we obtain for the total scattered field

$$E_{10y}^s = E_{y10}^+ \sum_{\text{Disks}} b_{10} = e_{10} e^{\Gamma_{10} z} \sum_{\text{Disks}} b_{10} \tag{19}$$

where the summation is taken over all disks in the waveguide cross section and e_{10} is given in (1).

The reflection coefficient for the TE_{10} mode is then found from

$$R_0 = \frac{E_{10y}^s(z=0)}{E_{10y}^i(z=0)} = -\frac{jkZ_0}{E_0}\left[\frac{2}{jghkZ_0\Gamma_{10}}\right]^{1/2} \sum_{\text{Disks}} b_{10}. \tag{20}$$

Using (15) and Eggimann,[1] we calculate the multipole moments. We obtain

$$P_y^1 = \frac{16}{3} a^3 \epsilon_0 E_0 \cos(k_x x_m) A_{ey}^1 \tag{21}$$

$$A_{ey}^1 = \left[1 + \frac{8}{15}(ka)^2 - \frac{1}{6}\sin^2\theta_i (ka)^2 - j\frac{8}{9\pi}(ka)^3\right]$$

$$M_z^1 = -\frac{16}{3} a^3 \frac{g}{j\omega\mu_0} E_0 \sin(k_x x_m) A_{mz}^1 \tag{22}$$

$$A_{mz}^1 = \frac{1}{2}\left[1 - \frac{2}{10}(ka)^2 - \frac{1}{10}\sin^2\theta_i (ka)^2 + j\frac{4}{9\pi}(ka)^3\right]$$

$$P_{yx}^2 = -\frac{16}{3} a^3 \frac{g}{\omega^2\mu_0} E_0 \sin(k_x x_m) A_{eyx}^2 \tag{23}$$

$$A_{eyx}^2 = \frac{2}{15}(ka)^2$$

$$Q_{zx} = \frac{16}{3} a^5 j\omega\mu_0 E_0 \cos(k_x x_m) A_{mzx}^2 \tag{24}$$

$$A_{mzx}^2 = \frac{1}{5}\left[(2 + \sin^2\theta_i) + \frac{1}{42}(52 - 16\sin^2\theta_i - 3\sin^4\theta_i) \cdot (ka)^2 - j\frac{20}{9\pi}(ka)^3\right]$$

$$P_{yxx}^3 = \frac{16}{3} a^5 \epsilon_0 E_0 \cos(k_x x_m) A_{eyxx}^3 \tag{25}$$

$$A_{eyxx}^3 = \frac{1}{5}\left[1 + \frac{1}{210}(110 - 47\sin^2\theta_i)(ka)^2 - j\frac{8}{9\pi}(ka)^3\right].$$

Substituting the values for E_{10}^+ and H_{10}^+ from (1) and (4) and (21) to (25) in (17) and performing the summation over the disks in the waveguide cross section, we obtain for the reflection coefficient

$$R_0 = -j\frac{8k^2a^3}{3cd\beta_{10}}\left[A_{ey}^1 - \left(\frac{\pi}{gk}\right)^2 A_{mz}^1 + \frac{1}{2}\left(\frac{\pi}{gk}\right)^2 A_{eyx}^2 - \frac{1}{3}\left(\frac{\pi e}{g}\right)^2 A_{mzx}^2 - \frac{1}{6}\left(\frac{\pi e}{g}\right)^2 A_{eyxx}^3\right]$$

$$= R' + jR'' \quad \text{for } m \neq 1 \tag{26}$$

(m = number of disks in the x direction)

where g/m and h/m have been replaced by c and d, the spacings between disks in the x and y directions, respectively.

For the case of a single disk (26) becomes

$$R_0 = -j\frac{16k^2a^3}{3cd\beta_{10}}\left(A_{ey}^1 + \frac{1}{2}\left(\frac{\pi}{gk}\right)^2 A_{eyx}^2 - \frac{1}{6}\left(\frac{\pi c}{g}\right)^2 A_{eyxx}^2\right). \tag{27}$$

In order to obtain a better approximation we now consider the interactions between the disks, and the disks and the guide walls. For the case of a free space array of dipoles this has been done by Collin and Eggimann.[7] They considered an incident plane wave given by

$$\boldsymbol{E}^i = E_y e^{-j(k_x x + \beta_{10} z)} \cdot \boldsymbol{a}_y \tag{28}$$

where $k_x = k \sin \theta_i$, $\beta_{10} = k \cos \theta_i$.

The induced dipole moments have a phase delay in the x direction given by $k_x c$. Due to the symmetry of the problem the induced electric dipole moment $\boldsymbol{P}$ has a y component only. In this case the interaction field at the center of a disk is found to be

$$\begin{aligned} E_y^{\text{int}} &= C_{ee} \frac{P_y}{\epsilon_0} + C_{em} Z_0 M_z^{\text{tot}} \\ H_z^{\text{int}} &= C_{me} Y_0 \frac{P_y}{\epsilon_0} + C_{mm} M_z^{\text{tot}}. \end{aligned} \tag{29}$$

The interaction constants C_{ee}, C_{em}, C_{me}, and C_{mm} are obtained by summing the contributions to the fields due to all electric and magnetic dipole moments and are given by

$$C_{ee} = \frac{1}{4\pi} \sum_{m=-\infty}^{\infty} \sum_{n=-\infty}^{\infty}{}' \left[2(1 + jkR)(nd)^2 - (1 + jkR - k^2R^2)(mc)^2\right] \frac{e^{-jkR - jk_x mc}}{R^5} \tag{30}$$

$$C_{em} = -\frac{k^2}{4\pi} \sum_{m=-\infty}^{\infty} \sum_{n=-\infty}^{\infty}{}' \frac{nd}{R^2} e^{-jkR - jk_x mc} \tag{31}$$

$$C_{me} = \frac{jk}{4\pi} \sum_{m=-\infty}^{\infty} \sum_{n=-\infty}^{\infty}{}' (1 + jkR) \frac{mc}{R^3} e^{-jkR - jk_x mc} \tag{32}$$

$$C_{mm} = -\frac{1}{4\pi} \sum_{m=-\infty}^{\infty} \sum_{n=-\infty}^{\infty}{}' (1 + jkR - k^2R^2) \frac{1}{R^3} e^{-jkR - jk_x mc} \tag{33}$$

where $R = [(mc)^2 + (nd)^2]^{1/2}$.

The prime on the summation sign indicates that the term $m = n = 0$ is to be omitted.

These sums can be written in the form of a rapidly converging series as follows:

$$\begin{aligned} C_{ee} = {} & \frac{1}{\pi d^3}\left[1.2 - \frac{k^2d^2}{2} \ln kd + \frac{k^2d^2}{4} + \frac{3k^4d^4}{288}\right] \\ & - \frac{k^2}{2cd}\left[\frac{c}{\pi}\left(\ln \frac{4}{kd} - \gamma\right) - \sum_{m=1}^{\infty}\left(\frac{1}{\Gamma_m} + \frac{1}{\Gamma_{-m}} - \frac{c}{\pi m}\right)\right] \\ & - \frac{2}{\pi d} \sum_{m=1}^{\infty} \sum_{n=1}^{\infty} \gamma_n^2 \cos(k_x mc) K_0(\gamma mc) \\ & + j\left[\frac{k^2}{2cd}\left(\frac{c}{2} - \frac{1}{(k^2 - k_x^2)^{1/2}}\right) - \frac{1}{\pi d^3}\left(\frac{\pi}{4} k^2d^2 - \frac{k^3d^3}{6}\right)\right] \end{aligned} \tag{34}$$

$$\begin{aligned} C_{me} = {} & \frac{k}{2\pi d}\left\{-j \frac{\pi}{c} \frac{k_x}{(k^2 - k_x^2)^{1/2}} \right. \\ & + \frac{\pi}{c} \sum_{m=1}^{\infty}\left[\frac{\left(\frac{2m\pi}{c} + k_x\right)}{\Gamma_m} - \frac{\left(\frac{2m\pi}{c} - k_x\right)}{\Gamma_{-m}}\right] \\ & \left. + 4 \sum_{m=1}^{\infty} \sum_{n=1}^{\infty} \gamma_n \cos(k_x mc) K_1(\gamma_n mc)\right\} \end{aligned} \tag{35}$$

$$C_{em} = C_{me} \tag{36}$$

$$\begin{aligned} C_{mm} = {} & -\frac{1}{2\pi d}\left\{\left[\frac{1.2}{d^2} + \frac{\pi^2}{3c^2} + \frac{k^2}{2}(1 - \gamma) + \frac{k^4d^2}{96} \right.\right. \\ & \left. + \frac{k^2}{2} \ln \frac{4\pi}{k^2cd} + k^2 \ln 2 \sin k \frac{d}{2}\right] \\ & - \frac{\pi}{c} \sum_{m=1}^{\infty}\left[\Gamma_m + \Gamma_{-m} - \frac{4m\pi}{c} + \frac{k^2c}{2m\pi}\right] \\ & - \frac{k^2\pi}{c} \sum_{m=1}^{\infty}\left[\frac{1}{\Gamma_m} + \frac{1}{\Gamma_{-m}} - \frac{c}{m\pi}\right)\Bigg] \\ & - 4k^2 \sum_{m=1}^{\infty} \sum_{n=1}^{\infty} \cos(k_x mc) K_0(\gamma_n mc) \\ & + \frac{4}{c} \sum_{m=1}^{\infty} \sum_{n=1}^{\infty} \cos(k_x mc) \frac{\gamma_n}{m} K_1(\gamma_n mc) \\ & \left. - j\left[\frac{k^3d}{3} - \frac{\pi k_x^2}{c(k^2 - k_x^2)^{1/2}}\right]\right\} \end{aligned} \tag{37}$$

where K_0 and K_1 are modified Bessel functions of the second kind.

$$\begin{aligned} \Gamma_m^2 &= \left(\frac{2m\pi}{c} + k_x\right)^2 - k^2 \\ \gamma_n^2 &= \left(\pi \frac{2n}{d}\right)^2 - k^2 \\ \gamma &= 0.577 = \text{Euler's constant.} \end{aligned} \tag{38}$$

If the disks are sufficiently far apart, *i.e.*, $kR \gg 1$, we can use a plane wave approximation and calculate the induced electric and magnetic dipole moment due to the interaction field. We obtain

$$P_y = \alpha_e \epsilon_0 E_y^{\text{int}} + \alpha_e^{\text{inc}} \epsilon_0 E_y^{\text{inc}} \tag{39}$$

$$M_z = \alpha_m H_z^{\text{int}} + \alpha_m^{\text{inc}} H_z^{\text{inc}}. \tag{40}$$

α_e^{inc} and α_m^{inc} are the electric and magnetic polarizabilities for the incident field and are obtained from A_{ey}^1 and A_{mz}^1 in (21) and (22).

$$\alpha_e^{\text{inc}} = \frac{16}{3} a^3 \left[1 + \left(\frac{8}{15} - \frac{1}{6} \sin^2 \theta_i\right)(ka)^2 - j \frac{8}{9\pi}(ka)^3\right] \tag{41}$$

$$\alpha_m^{\text{inc}} = -\frac{8}{3} a^3 \left[1 - \frac{1}{10}(2 + \sin^2 \theta_i)(ka)^2 + j \frac{8}{9\pi}(ka)^3\right]. \tag{42}$$

[7] R. E. Collin and W. H. Eggimann, "Dynamic interaction fields in a two-dimensional lattice," IRE TRANS. ON MICROWAVE THEORY AND TECHNIQUES, vol. MTT-9, pp. 110–115; March, 1961.

The electric and magnetic polarizabilities α_e and α_m for the interaction are obtained from (41) and (42) if we set $\theta_i = 90°$, because the direction of propagation of the interaction field is parallel to the plane of the disks.

Solving (29), (39) and (40) for the dipole moments yields

$$P_y = \frac{(1 - \alpha_m C_{mm})\alpha_e^{\text{inc}}\epsilon_0 E_y^{\text{inc}} + \alpha_e\alpha_m^{\text{inc}}\epsilon_0 C_{em} Z_0 H_z^{\text{inc}}}{(1 - \alpha_e C_{ee})(1 - \alpha_m C_{mm}) - \alpha_e\alpha_m C_{em}C_{me}} \quad (43)$$

$$M_z = \frac{(1 - \alpha_e C_{ee})\alpha_m^{\text{inc}} H_z^{\text{inc}} + \alpha_e^{\text{inc}}\alpha_m C_{me} Y_0 E_y^{\text{inc}}}{(1 - \alpha_e C_{ee})(1 - \alpha_m C_{mm}) - \alpha_e\alpha_m C_{em}C_{me}}. \quad (44)$$

In reality $\alpha_e C_{em}$ and $\alpha_m C_{me}$ are small compared with the other terms so that (43) and (44) reduce to

$$P_y = \frac{\alpha_e^{\text{inc}}\epsilon_0}{1 - \alpha_e C_{ee}} E_y^{\text{inc}} \quad (45)$$

$$M_z = \frac{\alpha_m^{\text{inc}}}{1 - \alpha_m C_{mm}} H_z^{\text{inc}}. \quad (46)$$

This means we neglect the interaction between electric and magnetic dipoles. For small spacings between the disks the plane wave approximation of the interaction field may be insufficient. In this case it is necessary to calculate the induced dipole moments on the disk due to a dipole field. This can be done by using the general expressions for the induced current distribution given by (33) and (34) in Eggimann.[1] The interaction can now be expressed by the equations

$$P_y^d = D_{ee} p_y \quad (47)$$

$$M_z^d = D_{mm} m_z \quad (48)$$

where

P_y^d = induced electric dipole moment due to the total field of all electric dipoles p_y,

M_z^d = induced magnetic dipole moment due to the total field of all magnetic dipoles m_z.

The new interaction constants are

$$D_{ee} = \alpha_e C_{ee} + \frac{4(ka)^5}{90} \sum_{m=-\infty}^{\infty} \sum_{n=-\infty}^{\infty}{}' \cdot \left\{ \left[\frac{36}{(kR)^5} + \frac{36j}{(kR)^4} - \frac{10}{(kR)^3} + \frac{2j}{(kR)^2} \right] - \left[\frac{45}{(kR)^7} + \frac{45j}{(kR)^6} - \frac{18}{(kR)^5} - \frac{3j}{(kR)^4} \right] (kmc)^3 \right\} \cdot e^{-jkR - jk_x mc}. \quad (49)$$

$$D_{mm} = \alpha_m C_{mm} + \frac{2(ka)^5}{30} \sum_{m=-\infty}^{\infty} \sum_{n=-\infty}^{\infty}{}' \cdot \left\{ \frac{7}{(kR)^5} + \frac{7j}{(kR)^4} - \frac{2}{(kR)^3} - \frac{j}{(kR)^2} \right\} \cdot e^{-jkR - jk_x mc}. \quad (50)$$

The summation terms represent corrections to the plane wave approximation. For large kR and $c \neq 0$ they are one order smaller than the leading terms $\alpha_e C_{ee}$ and $\alpha_m C_{mm}$. Their numerical computation is difficult because they converge very slowly if kR is not large. We can use, however, the same method as was employed for the evaluation of the interaction constants C_{ee} and C_{mm}.[7] There, a Fourier transform was used to obtain a rapidly convergent series for the field components, where only the first terms had to be calculated. Using the foregoing results, we finally obtain for the reflection coefficient ($m \neq 1$)

$$R_0 = -j \frac{8k^2a^2}{3cd\beta_{10}} \left[\frac{A_{ey}^1}{1 - D_{ee}} - \left(\frac{\pi}{gk}\right)^2 \frac{A_{mz}^1}{1 - D_{mm}} + \frac{1}{2}\left(\frac{\pi}{gk}\right)^2 A_{eyx}^2 - \frac{1}{3}\left(\frac{\pi c}{g}\right)^2 A_{mzx}^2 - \frac{1}{6}\left(\frac{\pi c}{g}\right)^2 A_{eyxx}^3 \right] \quad (51)$$

where $\alpha_e C_{ee}$ and $\alpha_m C_{mm}$ have been replaced by D_{ee} and D_{mm}, respectively.

No interaction between higher order multipole moments is taken into account in this equation.

The normalized shunt susceptance for the TE_{10} mode can now be readily evaluated from the relation

$$Y = G + jB = \frac{1 - R_0}{1 + R_0} = \frac{1 - R_0' - jR_0''}{1 + R_0' + jR_0''} \text{ at } z = 0. \quad (52)$$

Here we encounter, however, the difficulty to relate the calculated approximate values for G and B to the results of the experimental measurements. If we assume perfectly conducting disks, it is clear that no electromagnetic power will be absorbed by the disks. That in turn means that the disks represent a pure shunt susceptance in parallel with the characteristic admittance $Y = G = 1$ of the waveguide. If we calculate G and B from (52) we obtain

$$G = \frac{(1 - R_0'^2) - R_0''^2}{(1 + R_0')^2 + R_0''^2} \quad (53)$$

$$B = \frac{-2R_0''}{(1 + R_0')^2 + R_0''^2}. \quad (54)$$

If a rigorous solution for $R_0 = R_0' + jR_0''$ could be found, (53) should then be equal to 1. It seems now a good approximation to assume that B corresponds to the measured shunt susceptance as long as $G \simeq 1$. We can also plot R_0' vs R_0'' from (52) for the case $G = 1$ as shown in Fig. 3. We obtain

$$R_0' = \frac{-B^2}{4 + B^2} \quad (55)$$

$$R_0'' = \frac{2B}{4 + B^2}. \quad (56)$$

If the theoretical values for R_0' and R_0'' represent good approximations, the corresponding point in Fig. 3 should be close to the curve given by (55) and (56). We could further take the point on the curve which is closest to the calculated value Q and read the value for B from the graph. This, however, does not necessarily represent a better approximation than (54).

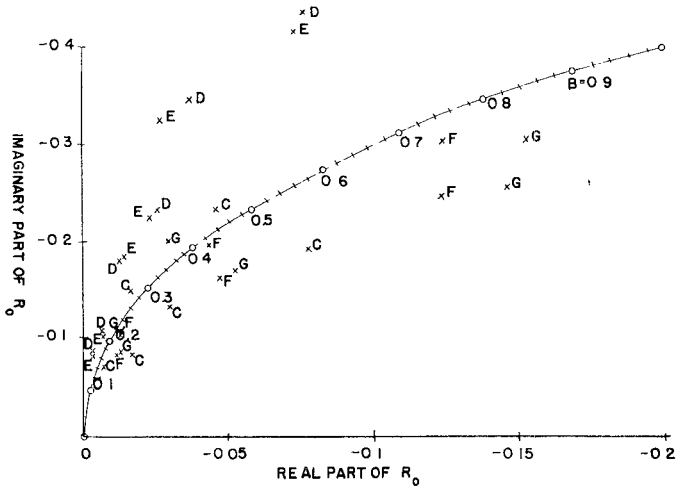

Fig. 3—Relation between the real and imaginary part of the reflection coefficient R_0 for a lossless shunt admittance in a waveguide as given by (55) and (56). The calculated points for a disk loaded waveguide are indicated.

Numerical Results

The preceding analysis will now be applied to the numerical evaluation of the input susceptance of a disk-loaded waveguide. Gardner[8] has obtained experimental results for the case of two, six and eight disks with different radii in a transverse plane of the guide. He then calculated the input susceptance in the first-order approximation with static and dynamic interaction between the disks. Unfortunately the seemingly more accurate results for dynamic interaction compared less favorably with the measurements.

We consider only the case of two disks in a standard size waveguide as shown in Fig. 4. The shunt susceptance will then be evaluated for three different radii ($a=0.1''$, $0.125''$, $0.15''$) and two different frequencies ($f=9$ kmc, 11 kmc). The following cases will now be considered:

1) No interaction between the disks. All higher order multipole moments are neglected. First-order approximation for the dipole moments. The reflection coefficient is given by

$$R_0 = -j\frac{8k^2a^3}{3cd\beta_{10}}\left\{1 - \frac{1}{2}\left(\frac{\pi}{gk}\right)^2\right\}. \tag{57}$$

[8] R. A. Gardner, "Shunt Susceptance of Planar Arrays of Conducting Disks," M.S. thesis, Case Inst. of Tech., Cleveland, Ohio, Sci. Rept. No. 13, AF 19(604)-3887; April, 1960.

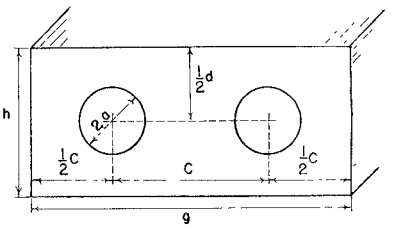

Fig. 4—Rectangular waveguide with two circular disks.

2) Static interaction between the disks. All higher order multipole moments are neglected. First-order approximation for dipole moments.

$$R_0 = -j\frac{8k^2a^3}{3cd\beta_{10}} \cdot \left\{\frac{1}{1-\alpha_e{}^B C_{ee}{}^s} - \frac{1}{2}\left(\frac{\pi}{gk}\right)^2 \frac{1}{1-\alpha_m{}^B C_{mm}{}^s}\right\}. \tag{58}$$

$C_{ee}{}^s$ and $C_{mm}{}^s$ are the static interaction constant which can be obtained from (34) and (37) by setting $k=0$.

$$\alpha_e{}^B = \frac{16}{3}a^3, \qquad \alpha_m{}^B = -\frac{8}{3}a^3$$

= polarizabilities calculated by Bethe.

3) Dynamic interaction in plane wave approximation between the disks. All higher order multipole moments are neglected. First-order approximation for dipole moments.

$$R_0 = -j\frac{8k^2a^3}{3cd\beta_{10}} \cdot \left\{\frac{1}{1-\alpha_e{}^B C_{ee}} - \frac{1}{2}\left(\frac{\pi}{gk}\right)^2 \frac{1}{1-\alpha_m{}^B C_{mm}}\right\} \tag{59}$$

where C_{ee} and C_{mm} are given in (34) and (37).

4) No interaction between the disks. All higher order multipole moments are neglected. Third-order approximation for dipole moments.

$$R_0 = -j\frac{8k^2a^3}{3cd\beta_{10}}\left\{A_{ey}{}^1 - \left(\frac{\pi}{gk}\right)^2 A_{mz}{}^1\right\}. \tag{60}$$

$A_{ey}{}^1$ and $A_{mz}{}^1$ are given in (21) and (22).

5) No interaction between the disks. Higher order multipole moments are considered. Third-order approximation for multipole moments.

$$R_0 = -j\frac{8k^2a^3}{3cd\beta_{10}} \cdot \left\{A_{ey}{}^1 - \left(\frac{\pi}{gk}\right)^3 A_{mz}{}^1 + \frac{1}{2}\left(\frac{\pi}{gk}\right)^2 A_{cyx}{}^2 - \frac{1}{3}\left(\frac{\pi c}{g}\right)^2 A_{mzx}{}^2 - \frac{1}{6}\left(\frac{\pi c}{g}\right)^2 A_{eyxx}{}^3\right\}. \tag{61}$$

The coefficients $A_{rst}{}^n$ are given in (21) to (25).

6) Dynamic interaction in plane wave approximation between the dipole moments of the disks. Higher order multipole moments are considered. Third-order approximation for multipole moments.

$$R_0 = -j\frac{8k^2a^3}{3cd\beta_{10}} \cdot \left\{\frac{A_{ey}{}^1}{1-\alpha_e C_{ee}} - \left(\frac{\pi}{gk}\right)^2 \frac{A_{mz}{}^1}{1-\alpha_m C_{mm}} + \frac{1}{2}\left(\frac{\pi}{gk}\right)^2 A_{eyx}{}^2 - \frac{1}{3}\left(\frac{\pi c}{g}\right)^2 A_{mzx}{}^2 - \frac{1}{6}\left(\frac{\pi c}{g}\right)^2 A_{eyxx}{}^3\right\}. \quad (62)$$

α_e and α_m are given in (41) and (42) for $\theta: \doteq 90°$.

7) Dynamic interaction in dipole wave approximation between the dipole moments of the disks. Higher order multipole moments are considered. Third-order approximation for the multipole moments.

$$R_0 = -j\frac{8k^2a^3}{3cd\beta_{10}} \cdot \left\{\frac{A_{ey}{}^1}{1-D_{ee}} + \left(\frac{\pi}{gk}\right)^2 \frac{A_{mz}{}^1}{1-D_{mm}} + \frac{1}{2}\left(\frac{\pi}{gk}\right)^2 A_{eyx}{}^2 - \frac{1}{3}\left(\frac{\pi c}{g}\right)^2 A_{mzx}{}^2 - \frac{1}{6}\left(\frac{\pi c}{g}\right)^2 A_{eyxx}{}^3\right\}. \quad (63)$$

D_{ee} and D_{mm} are defined in (49) and (50).

Numerical calculations for the input susceptance as given by (54) have been carried out for the following values:

$c = 0.0114$ meter

$d = 0.0102$ meter

$g = 0.0228$ meter

$h = 0.0102$ meter

$a = 0.00254, 0.00318, 0.00381$ meter

$f = 9, 11$ Gc

$k = 189, 230$ (meter)$^{-1}$

$\beta_{10} = 130, 184$ (meter)$^{-1}$

$k_x = 138$ (meter)$^{-1}$.

The interaction constants D_{ee} and D_{mm} have been calculated by using a digital computer. In Fig. 5(a) and (b) the input susceptance B has been plotted as a function of the important quantity (ka) for the two different frequencies. Each graph shows the seven different theoretical approximations listed above. The thicker solid line represents the experimental results.

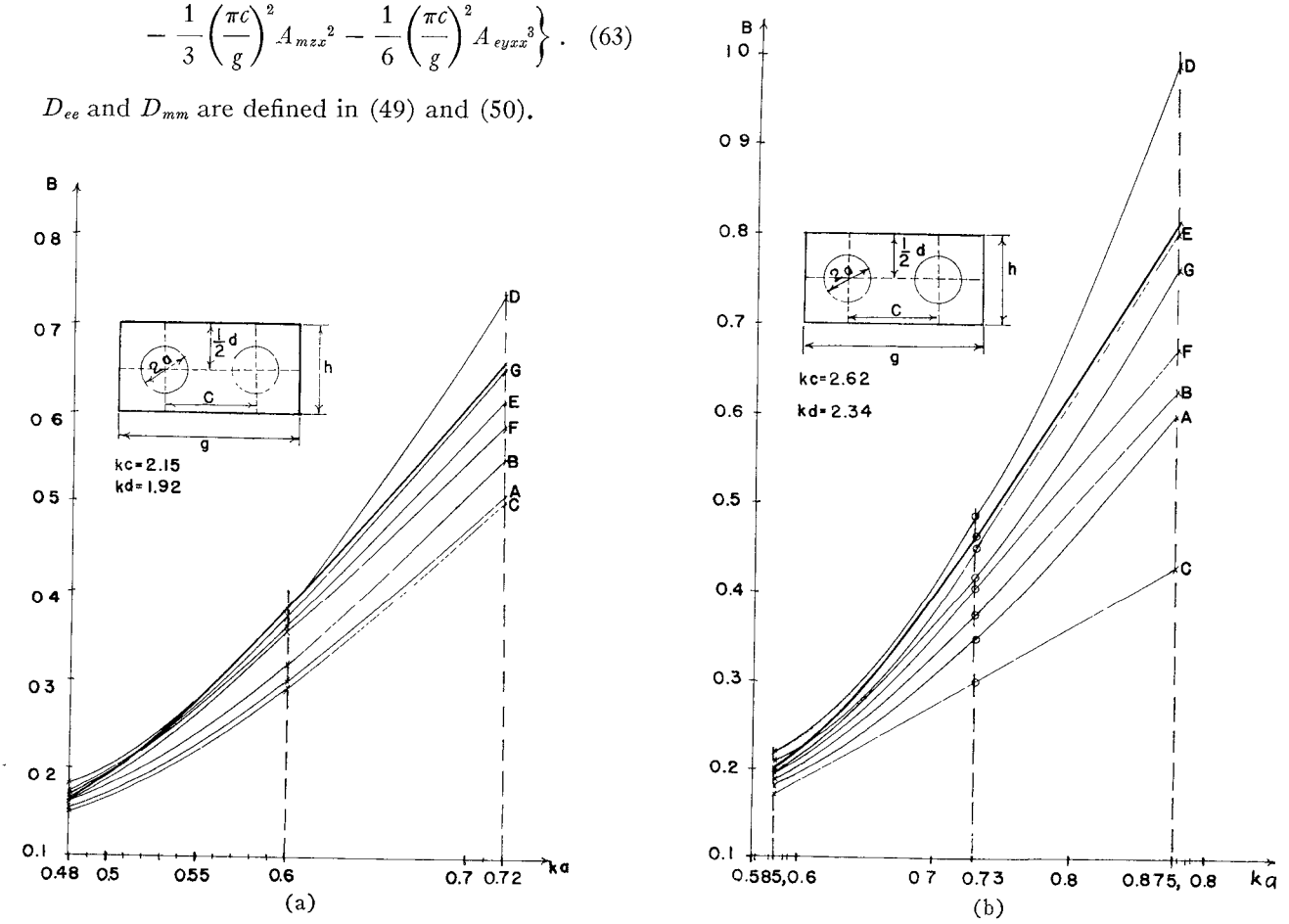

Fig. 5—(a) Input susceptance of a disk loaded rectangular waveguide for different disk radii a. Frequency $f=9$ Gc. (b) Input susceptance of a disk loaded rectangular waveguide for different disk radii a. Frequency $f=11$ Gc.

Discussion and Conclusion

For a detailed discussion of the method which was used to measure the equivalent input susceptance of the disks the reader is referred to the original report.[4] Extreme care was taken in manufacturing the disks and in placing them at the desired location within the waveguide. A polyfoam support of low dielectric constant ($k=1.05$), was used and its calculated and measured equivalent susceptance was subtracted from the final measurements. The estimated error should not exceed one or two per cent.

From the few numerical data available (theoretical and experimental) it is not possible to draw conclusions which are valid for every general case. It is, however, clear that the simple dipole approximation of Bethe gives reliable results only for rather small disk radii of the order less than $\frac{1}{10}$ of a wavelength ($ka<0.5$). It is interesting to note that the dynamic interaction calculation C does not improve the result; on the contrary, the values obtained are much too small. The dynamic interaction calculation seems to give also a lower value for the susceptance, if the curves E and F are compared. Generally it is observed that consideration of static interaction increases the susceptance, dynamic interaction decreases the susceptance, higher order calculations increase the susceptance, higher order multipole moments decrease the susceptance, dipole wave interaction gives a higher susceptance than plane wave interaction.

It should be emphasized that all our results are obtained for comparatively short separation distances s in the order of $(ks)\sim 2.5$. For other values the remarks above might not be valid.

Which approximation should be used for each case is not easy to decide without some more numerical data. It seems, however, that even for closely spaced disks, where the spacing is only a few multiples of the disk radius, it is just as important to obtain a more accurate representation of the diffraction field for a single disk as it is to obtain the interaction between the disks.

If only dipole moments in the third-order approximation are considered D, the value for B turns out to be too large. Higher order multipoles, however, seem to give values which are very close to the experimental results. Interaction calculations between the disks in the dipole wave approximation G give better results in all cases compared to the plane wave interaction F. However, it is somewhat surprising and paradoxical, that in some cases they do not seem to give an improvement over cases where no interaction is considered. This is shown in Fig. 5(b), where the curve E is closer to the measured points than the curve G. An explanation might be found from Fig. 3 where the results for the reflection coefficients $R_0=R_0'+jR_0''$ are plotted. As mentioned before, these points should lie on the solid curve if the disks are lossless. The distance of the points from the curve thus gives us a measure of the consistency of our calculations.

From (51) it is clear that the results A and B are purely imaginary and are therefore the least consistent ones. C is quite consistent but it does not compare very well with the experimental results in Fig. 5(b). D and E are comparatively inconsistent, where D does not agree with experiments while E does so quite well. F and G are about equally consistent but G compares better with the measurements. In terms of over-all accuracy it seems that the most sophisticated calculation G gives also the best agreement with experiments.

Comparing the different disk radii we can draw the following conclusions for our disk separation $s\sim 2.5/k$:

Bethe Theory is applicable for	$(ka)<0.5$
Third-Order Theory is applicable for	$(ka)<0.9$
Higher order multipoles have to be considered for	$(ka)>0.6$
Static interaction is necessary for	$(ka)>0.5$
Dynamic interaction in dipole field approximation is needed for	$(ka)>0.7$.

The dynamic interaction in the plane wave approximation gives only an improvement if the separation of the disks is larger than the one considered here, probably for values of the order of $(ks)>6$.

For larger disks higher order calculations would have to be made and for small spacings the interaction between higher order multipole moments will become important.

The calculations as described in this paper can in principle be extended to achieve any degree of accuracy. It seems, however, that for values $(ka)>1$ the calculations become so laborious as to be impractical. On the other hand, it would be very desirable to obtain more numerical data for the region of $(ka)<1$ and a wider range of spacings between the disks in order to decide which approximation is the most suitable for a particular problem.